NASA Contractor Report 194897

ICASE Report No. 94-19

ICASE

THE EFFECT OF CROSSFLOW ON GÖRTLER VORTICES

S. R. Otto
James P. Denier

Contract NAS1-19480
March 1994

Institute for Computer Applications in Science and Engineering
NASA Langley Research Center
Hampton, VA 23681-0001

Operated by Universities Space Research Association

ICASE Fluid Mechanics

Due to increasing research being conducted at ICASE in the field of fluid mechanics, future ICASE reports in this area of research will be printed with a green cover. Applied and numerical mathematics reports will have the familiar blue cover, while computer science reports will have yellow covers. In all other aspects the reports will remain the same; in particular, they will continue to be submitted to the appropriate journals or conferences for formal publication.

THE EFFECT OF CROSSFLOW ON GÖRTLER VORTICES

S. R. Otto[1]
School of Mathematics and Statistics
University of Birmingham
Edgbaston
Birmingham, B15 2TT
United Kingdom
and
James P. Denier[2]
School of Mathematics
University of New South Wales
P.O. Box 1
Kensington, NSW 2033
Australia

ABSTRACT

It is well known that the boundary layer flow over a surface with a region of concave curvature is susceptible to centrifugal instabilities in the form of Görtler vortices. In the limit of large Görtler number (a parameter which is a measure of the curvature of the surface) the effect of a crossflow component in the underlying basic flow has been shown to stabilises these modes and thus render the Görtler vortex mechanism inoperable in these situations. Here we consider the effect of crossflow when the Görtler number (and the scaled spanwise wavenumber of the vortex) are both order one quantities. The parabolic partial differential equations governing the linear evolution of a Görtler vortex in a three-dimensional boundary layer are solved numerically. Our results suggest that, at least for small magnitude crossflows, the Görtler vortex instability mechanism is still operable. In addition we consider the effect of an applied pressure gradient within the boundary layer on the instability mechanism and demonstrate that a favourable pressure gradient renders the boundary layer more susceptible to the Görtler vortex instability; this is in stark contrast to the case of Tollmien-Schlichting waves where a favourable pressure gradient stabilises the flow.

[1]This research was supported by the National Aeronautics and Space Administration under NASA Contract No. NAS1-19480 while the first author was in residence at the Institute for Computer Applications in Science and Engineering (ICASE), NASA Langley Research Center, Hampton, VA.
[2]This research was supported by the Australian Research Council.

§1 Introduction

There are many mechanisms which can promote transition in a boundary layer and as such it is important to be able to predict how a given physical characteristic will effect the breakdown of the flow. Our concern is with the problem of how two such features will compete to change the transition characteristics of the flow. The two features considered here are crossflow and the concave curvature of the plate.

Many physical situations have flow components in more than one direction, one example being the boundary layer flow over a swept wing. In such a geometry there is a flow parallel to the leading edge as well as along the wings chord. In flight experiments Gray (1952) noted that a swept wing boundary layer reaches a transition stage far earlier than its two-dimensional counterpart. The explanation of this was given by Gregory, Stuart, & Walker (1955), who studied the archetypical three–dimensional boundary layer above a rotating disc. By considering this problem from both a theoretical and experimental standpoint they were able to demonstrate the existence of, what are now known as, crossflow vortices. In addition to crossflow the boundary layer flow over a swept wing also brings forward the question of how an applied pressure gradient will affect the flows stability.

In the seminal work of Taylor (1923) it was shown that centrifugal forces could support a toroidal vortex state in the fluid filled gap between two concentric cylinders. Those ideas were extended by Görtler (1940) and applied to the case of an external boundary layer flow. The results of this study demonstrated that the flow over a concave plate perpendicular to its generator is susceptible to a longitudinal vortex state. Such instabilities are due to the centrifugal forces present in situations where wall curvature is present. Since the initial work of Taylor (1923) and Görtler (1940) the centrifugal instability problem has attracted much attention, and has been studied both experimentally and theoretically, using mixture of asymptotic and numerical techniques.

It is now known that the Görtler vortex instability mechanism is a truly non–parallel phenomena, in that it is not possible to predict a growth rate locally independent of the upstream history of the disturbance. The modes initial form and the position at which it is imposed both play a significant role in the evolution of the mode. The work of Hall (1983) represents the first attempt at solving the correct equations governing this vortex state. A Görtler vortex varies over commensurate scales in the wall normal and spanwise directions, but evolves on the same scale as the underlying boundary layer evolves in the streamwise coordinate. Thus in the limit of large Reynolds the

streamwise derivative of the pressure and the streamwise diffusion terms do not enter into the governing equations. However, the streamwise derivatives in the convective terms cannot be neglected as they are the same order of magnitude as the wall normal and spanwise terms, due to the size of the convective velocities in these directions. Thus the terms that can legitimately be removed render the system parabolic in the streamwise coordinate, and hence enable its solution by a relatively cheap marching procedure from some given streamwise location with some prescribed initial form. This initial form must be consistent with the governing equations which impose conditions on the normal structure of the disturbance; these conditions are derived in a similar way to those given in Goldstein's (1948) study of a flow near a point of separation. The parabolic equations can then be marched forward and the magnitude of the mode monitored; when the streamwise derivative of some suitable norm of the mode becomes zero the mode is said to be at its neutral location. The concave curvature of the wall is allowed to vary with the distance from the leading edge, and the magnitude of the curvature is chosen so that the Görtler mechanism is operable. In Hall (1983) it was shown that as Görtler vortices progress downstream in order for them to be 'maintained' the wall must have curvature proportional to the square root of the distance from the leading edge. It was observed that as the calculation progresses the growth rate curves coalesce, as was noted and exploited in Hall (1982).

In an asymptotic study, assuming large Görtler number (corresponding to the behaviour far downstream) Hall (1985) showed that a crossflow will stabilise these modes. In that study far larger crossflows can be described, for instance Hall (1985) makes predictions concerning the effect of increasing the crossflow beyond the $O(R_e^{-1/2})$ bound, which will be imposed in the current study. (Here R_e is the, large, Reynolds number of the flow). In Hall (1985) an eigenvalue problem was derived which allowed the Görtler number required for neutrality to be found. As the degree of crossflow increases the Görtler number is modified and the vortex activity is driven to a thin wall layer, until it is ultimately extinguished. This behaviour has also been found theoretically in the narrow gap Taylor problem by Otto & Bassom (1994a). It was found that a smaller crossflow component is required to stabilise the most unstable Taylor vortex mode than the most unstable Görtler modes, so it was conjectured that the Görtler mechanism would be more prevalent in a mixed situation.

In a preliminary report Otto & Denier (1993a), (henceforth referred to as OD), we have shown that crossflow modifies the stability characteristics of Görtler vortices. In that study several assumptions were made in order to reduce the dimension of the parameter space. It will be shown that the results obtained in OD can be in

agreement with the earlier asymptotic results of Hall (1985), depending on the choice of the frequency of the modes, even for the small crossflows considered here.

The physical problem that we shall consider herein is the flow over a yawed cylinder where the surface of the body possesses a degree of concave curvature. The problem is non-dimensionalised in the normal manner, using the dimensional values U_∞ (a characteristic free-stream velocity), L (a characteristic lengthscale) and ν (the kinematic viscosity). There are two key non-dimensional parameters,

$$R_e = \frac{U_\infty L}{\nu}, \qquad G = 2R_e^{\frac{1}{2}}\delta, \tag{1.1}$$

the former being the Reynolds number which is assumed to be large, and the latter the Görtler number which is assumed to be an order one quantity. The value of δ, a curvature parameter, is chosen to tend to zero as $R_e \to \infty$ such that the G remains of order one, this ensures that the Görtler mechanism is operational. For a comprehensive review of the work on Görtler vortices the reader is referred to Hall (1990). In Bassom & Hall (1991) a study was made of the connection between crossflow and Görtler vortices within the high Görtler number regimes. The problem concerning the effect of crossflow on the Taylor modes was discussed by DiPrima & Pridor (1979).

In the work of Hall (1983) the growth of Görtler vortices within a Blasius boundary layer were considered. It is well known that the flow over a flat plate is self similar in the downstream coordinate, x; at least for large values of x or the Reynolds number. In the case of the flow over a swept wing there is a natural pressure gradient present and it is for this reason we shall consider first the effect of this pressure gradient on the stability characteristics of Görtler vortices. In OD it was shown that a favourable pressure gradient promotes the instability mechanism and is was conjectured that this is connected with the convective nature of the Görtler modes. We will assume that the pressure gradient takes the form x^{2n}, so that in the free stream the scaled streamwise velocity takes the form x^n. This form of the pressure gradient leads to the Falkner-Skan family of velocity profiles (Falkner & Skan (1930)). It is, of course, possible for other forms of pressure gradient to be used but these would only serve to complicate the problem so as to cloud the pertinent issues. In the work of Cooke (1950) the effect of yawing on this problem was considered and it was found that the spanwise momentum equation could be solved after obtaining the streamwise profile. The degree of crossflow has a direct correspondence with the angle of sweep.

After the momentum equations have been linearized about the basic state we have four coupled partial differential equations to solve. It is not clear how to impose boundary conditions on the perturbation pressure in this primitive formulation, so it is found to be convenient to eliminate the vortex spanwise velocity and pressure components. We first Fourier decompose in the spanwise direction (where the spanwise wavelength has been scaled on the boundary layer thickness) and assume that the modes are harmonic in the temporal variable (we note that it is beyond the scope of the calculations to be presented here to consider modes which evolve both temporally and spatially). The resulting equations then form a coupled system of partial differential equations for the velocity components as functions of the normal and streamwise variables. These equations are then discretized using a second order accurate finite difference scheme in the normal variable and a Crank–Nicholson scheme in the streamwise coordinate. A stretched grid is employed in the normal coordinate so as to retain adequate resolution near the wall without using prohibitively many points to obtain a sufficiently large outer bound for the calculations. The resulting discretized system is in the form of a coupled penta– and tri-diagonal system which was inverted directly at each streamwise location by using a modified form of a Davis Coupled scheme. This scheme has the advantage of directly inverting the system (thus yielding a true implicit scheme) without incurring the extra computational costs in inverting a full block system. This method was developed for a weakly nonlinear calculation, Bassom & Otto (1993), and has been shown to be efficient in other more complex calculations. The additional work involved in implementing the Crank–Nicholson scheme for the streamwise coordinate was minimal and did lead to improved accuracy when compared to the results obtained using a Backward Euler discretisation in the streamwise direction. As a test, consistency was demonstrated between the Euler results with a smaller step–size and the Crank-Nicholson results. The method used to invert the system is totally implicit; as such the streamwise step is restricted to be Δy rather than Δy^2 as it would be in an explicit scheme. However since both the Euler and Crank-Nicholson schemes are unconditionally stable, it is possible to use a larger streamwise steplength without invalidating our results.

Many of the conclusions found here have also been observed in a concurrent study by Zurigat & Malik (1993). That work concerns steady modes in situations with favourable pressure gradients. The study exploits a parallel flow approximation, which although erroneous, shows the link between Görtler modes and crossflow modes in three-dimensional boundary layers. In the context of our calculation it is not possible to describe the crossflow modes (Gregory, Stuart & Walker (1955)) due to the fact that

the streamwise derivatives that have been removed will become significant in such a problem.

The paper is organized as follows: in section 2 we derive the governing equations and discuss the conditions used to derive the initial conditions for the calculation. In section 3 we discuss the numerical techniques used to advance the solution. Section 4 contains a summary of the results, section 5 includes some conclusions and possible future extensions to this work and in an appendix we present some asymptotic results concerning the effect of pressure gradient on the Görtler instability mechanism.

§2 Formulation

We consider the flow over a yawed cylinder as described in Hall (1985) in which the body is assumed to have concave curvature perpendicular to its generator. Such a flow can support centrifugal instabilities and we wish to consider the effect of the angle of sweep, which has a direct correspondence to the amount of crossflow present in the unperturbed flow field, on the instability. We assume that the pressure gradient present in the flow is of a form which is conducive to a self similar calculation, namely x^{2n}. Since $\tilde{p} \sim x^{2n}$, the scaled velocity at the extreme edge of the boundary layer is given by $\bar{u}_e \sim x^n$, (from the balance $\bar{u}_e \bar{u}_{ex} = -\tilde{p}_x$). The viscous boundary layer then grows as $x^{\frac{1-n}{2}}$, and we introduce the similarity variable $\eta = y/x^{\frac{1-n}{2}}$, where y is the usual scaled boundary layer normal variable. Within the boundary layer the flow then takes the form

$$\left(\bar{u}, R_e^{-\frac{1}{2}}\bar{v}, R_e^{-\frac{1}{2}}\bar{w}\right) = \left(x^n f_\eta, R_e^{-\frac{1}{2}} x^{\frac{n-1}{2}} \left(\frac{1-n}{2}\eta f_\eta - \frac{1+n}{2} f\right), R_e^{-\frac{1}{2}} g\right), \qquad (2.1)$$

where the functions of η, f and g satisfy,

$$f_{\eta\eta\eta} + \frac{1+n}{2} f f_{\eta\eta} = n\left(f_\eta^2 - 1\right), \qquad g_{\eta\eta} + \frac{1+n}{2} f g_\eta = 0, \qquad (2.2a, b)$$

together with the boundary conditions

$$f = f_\eta = g = 0 \quad \text{at} \quad \eta = 0, \qquad f_\eta \to 1, g \to \lambda \quad \text{as} \quad \eta \to \infty.$$

If $\lambda = 0$ these equations give the standard Falkner-Skan boundary layer profile. In the case $n = 0$ we revert to the Blasius profile in which case g is a linear multiple of f and the Görtler vortex instability mechanism reverts to that for the two dimensional boundary layer flow over a curved plate (the reader is referred to Hall (1985) for a discussion of this case).

We assume that the bounding surface has curvature distribution of the form $\chi(x)$, where χ is a positive quantity for a concave wall. Hall (1982) noted that, for the case of a Blasius boundary layer, in order to support Görtler vortices far downstream of the leading edge we have the requirement that $\chi \sim x^{\frac{1}{2}}$. In the current problem this condition is now modified to be $\chi \sim x^{\frac{1-5n}{2}}$, which is readily deduced from the balances required near the right-hand branch of the neutral curve.

In this paper we restrict our attention to linear disturbances to the three-dimensional boundary layer. We perturb the basic state (2.1) with a small amplitude wave so that the total flow is now written as

$$\mathbf{q} = \left(\bar{u}, R_e^{-\frac{1}{2}}\bar{v}, R_e^{-\frac{1}{2}}\bar{w}, \tilde{p} + R_e^{-1}\bar{p}\right) + \Delta\left(\tilde{U}, R_e^{-\frac{1}{2}}\tilde{V}, R_e^{-\frac{1}{2}}\tilde{W}, R_e^{-1}\tilde{P}\right).$$

Substituting the above expansion into the incompressible, unsteady Navier–Stokes equations fitted to the plate, taking first the limit $\Delta \to 0$ and then the limit $R_e \to \infty$ we obtain the following system of viscous equations governing the evolution of a small amplitude disturbance:

$$\mathcal{L}\tilde{U} = \tilde{U}\frac{\partial \bar{u}}{\partial x} + \tilde{V}\frac{\partial \bar{u}}{\partial y}, \tag{2.3a}$$

$$\mathcal{L}\tilde{V} = \tilde{U}\frac{\partial \bar{v}}{\partial x} + \tilde{V}\frac{\partial \bar{v}}{\partial y} + G\chi\bar{u}\tilde{U} + \frac{\partial \tilde{P}}{\partial y}, \tag{2.3b}$$

$$\mathcal{L}\tilde{W} = \tilde{U}\frac{\partial \bar{w}}{\partial x} + \tilde{V}\frac{\partial \bar{w}}{\partial y} + \frac{\partial \tilde{P}}{\partial z}, \tag{2.3c}$$

$$\frac{\partial \tilde{U}}{\partial x} + \frac{\partial \tilde{V}}{\partial y} + \frac{\partial \tilde{W}}{\partial z} = 0. \tag{2.3d}$$

Here the differential operator $\mathcal{L}$ is given by

$$\mathcal{L} \equiv \frac{\partial^2}{\partial y^2} + \frac{\partial^2}{\partial z^2} - \bar{u}\frac{\partial}{\partial x} - \bar{v}\frac{\partial}{\partial y} - \bar{w}\frac{\partial}{\partial z} - \frac{\partial}{\partial t},$$

and, anticipating the well known result that the vortex wavelength scales on the boundary layer thickness, we have introduced the nondimensional variable $z = R_e^{1/2}z^*/L$. The boundary conditions appropriate to (2.3) are

$$\tilde{U} = \tilde{V} = \tilde{W} = 0 \quad \text{at} \quad y = 0, \infty, \tag{2.4}$$

corresponding to the requirement of no-slip at the wall and that the vortex is confined to the boundary layer.

At this juncture we note there is no streamwise derivative of the perturbation pressure and no streamwise diffusion in the perturbations equations (2.3) thus rendering the system parabolic in the streamwise coordinate x. As such the system (2.3) can be marched downstream with some suitable initial conditions imposed at $x = \bar{x}$ (say). However, as noted by Hall (1983) it is not sufficient to choose an initial form for the perturbation velocity fields which solely satisfies the boundary conditions (2.4); such a choice necessarily introduces singularities at $x = \bar{x}$. Indeed, the initial perturbation quantities must satisfy conditions stronger than (2.4) which can readily be derived by following the method outlined in Goldstein (1948) and expanding both $\tilde{U}$ and $\tilde{V}$ in Taylor series about $x = \bar{x}$. Such a procedure yields the result that the initial perturbations $\tilde{U} = \bar{U}(y)$ and $\tilde{V} = \bar{V}(y)$ must satisfy

$$\bar{U}_{yy}(0) = 0, \quad \bar{U}_{yyy}(0) = \left(a^2 + i\Omega\right)\bar{U}_y(0), \quad \bar{V}_{yyyy}(0) = \left(2a^2 + i\Omega\right)\bar{V}_{yy}(0), \quad (2.5)$$

in addition to the boundary conditions (2.4). Hall (1983) derives the condition that $\tilde{U}$ must satisfy as $Y \to \infty$, which when modified to account for the presence of the pressure gradient becomes

$$\tilde{U} \sim \exp\left(-\frac{y^2}{x^{1-n}}\frac{1+n}{4}\right). \quad (2.6)$$

As noted by Hall (1983) a parallel–flow approximation, in which the term $\bar{u}\partial_x$ is neglected, yields the large y structure

$$\tilde{U} \sim \exp(-ay),$$

thus predicting an incorrect decay in the far field for the perturbation quantities. It is for precisely this reason that the parallel flow approximation is erroneous in the context of the Görtler vortex problem.

In order to reduce the system (2.3) to a form which is more convenient from a computational standpoint we first Fourier decompose in the spanwise and temporal variable such that $\partial_z \to ia$ and $\partial_t \to -i\Omega$, where both a and Ω are real quantities, and eliminate the perturbation pressure and spanwise velocity perturbation to give

$$\begin{aligned}
&\mathcal{L}\left(\frac{\partial^2}{\partial y^2} - a^2\right)\tilde{V} + Ga^2\chi\bar{u}\tilde{U} + 2\frac{\partial^2\tilde{U}}{\partial x\partial y}\frac{\partial\bar{u}}{\partial x} + 2\frac{\partial\tilde{U}}{\partial x}\frac{\partial^2\bar{u}}{\partial x\partial y} \\
&+ \tilde{U}\frac{\partial^3\bar{u}}{\partial x^2\partial y} + \frac{\partial\tilde{V}}{\partial x}\frac{\partial^2\bar{u}}{\partial y^2} + \frac{\partial\tilde{V}}{\partial y}\frac{\partial^2\bar{u}}{\partial x\partial y} \\
&+ \tilde{V}\frac{\partial^3\bar{u}}{\partial x\partial y^2} + \frac{\partial\bar{v}}{\partial x}\frac{\partial^2\tilde{U}}{\partial y^2} + 2ia\frac{\partial^2\bar{w}}{\partial x\partial y}\tilde{U} + 2ia\frac{\partial\bar{w}}{\partial x}\frac{\partial\tilde{U}}{\partial y} \\
&- \frac{\partial\bar{v}}{\partial y}\frac{\partial^2\tilde{V}}{\partial y^2} + ia\tilde{V}\frac{\partial^2\bar{w}}{\partial y^2} + a^2\tilde{U}\frac{\partial\bar{v}}{\partial x} + a^2\tilde{V}\frac{\partial\bar{v}}{\partial y} = 0,
\end{aligned} \quad (2.7)$$

together with equation (2.3a), where the differential operator $\mathcal{L}$ is now given by

$$\mathcal{L} \equiv \frac{\partial^2}{\partial y^2} - a^2 - \bar{u}\frac{\partial}{\partial x} - \bar{v}\frac{\partial}{\partial y} - ia\bar{w} + i\Omega.$$

The problem now reduces to the numerical solution of the governing equations (2.3a) and (2.7) subject to the boundary conditions

$$\begin{aligned} &\tilde{U} = \tilde{V} = \frac{\partial \tilde{V}}{\partial y} = 0 \quad \text{at} \quad y = 0, \\ &\tilde{U}, \tilde{V}, \frac{\partial \tilde{V}}{\partial y} \to 0 \quad \text{as} \quad y \to \infty. \end{aligned} \tag{2.7}$$

given some initial perturbation at $x = \bar{x}$, consistent with the conditions (2.5) and (2.6), marching downstream in x. In the next section we present such a numerical procedure.

§3 Numerical Methods

The method used to numerically integrate the governing equations (2.3a) and (2.7) parallels that used by Hall (1983), however as there are some significant differences we now give an indication of the pertinent points regarding our numerical scheme.

Following Hall (1983) we elect to solve the system in terms of the similarity variable $\eta = y/x^{\frac{1-n}{2}}$. We then write $\tilde{U} = \tilde{U}(x, \eta)$, together with similar expressions for the vertical component of the perturbation velocity field, and take our underlying boundary layer flow to be described by (2.2a,b). The system can then be transformed from the (x, y)–space to the (x, η)–space by using the fact that

$$\frac{\partial}{\partial x} \to \frac{\partial}{\partial x} - \frac{1+n}{2}\frac{\eta}{x}\frac{\partial}{\partial \eta}, \qquad \frac{\partial}{\partial y} \to \frac{1}{x^{\frac{1-n}{2}}}\frac{\partial}{\partial \eta};$$

the higher order derivatives transform in a similar way as

$$\partial^2_{yy} = \frac{1}{x^{1-n}}\partial^2_{\eta\eta}, \qquad \partial^3_{yyy} = \frac{1}{x^{\frac{3-3n}{2}}}\partial^3_{\eta\eta\eta},$$

$$\partial^2_{xy} = \partial^2_{yx} = -\frac{1-n}{2}\frac{1}{x^{\frac{3-n}{2}}}\left(\partial_\eta + \eta\partial^2_{\eta\eta}\right) + \frac{1}{x^{\frac{1-n}{2}}}\partial^2_{\eta x},$$

$$\partial^3_{xyy} = -\frac{1-n}{2}\frac{1}{x^{2-n}}\left(2\partial^2_{\eta\eta} + \eta\partial^3_{\eta\eta\eta}\right) + \frac{1}{x^{1-n}}\partial^3_{\eta\eta x}.$$

Such a transformation allows the calculation to spread in the normal extent with the growth of the boundary layer. In order to achieve adequate resolution at the wall,

whilst still retaining a sufficiently large outer bound for the calculations and without using a prohibitively large number of normal grid–points, an algebraic stretching of the form introduced by Macaraeg, Streett & Hussaini (1988) was used for the η grid. In the majority of the calculations presented herein 150 points were used in the normal coordinate, with an outer bound at $\eta = 20$. The basic flow quantities $\bar{u}, \bar{v}$ and $\bar{w}$ were obtained *a priori* by using a standard fourth order Runge–Kutta technique, coupled to a two–dimensional real secant method, to integrate the similar equations (2.2); these were then projected onto the similarity grid at each downstream station.

In order to march the equations downstream from an initial position $x = \bar{x}$ a, formally second order accurate, Crank-Nicholson scheme was used in the downstream coordinate. If we compare this scheme with a Backward–Euler scheme, this being the method used by Hall (1983) and others, we find that in using the two schemes for $\frac{\partial \phi}{\partial x} + \frac{\partial^p \phi}{\partial y^p} = 0$, we are required to solve

Backward-Euler:

$$\frac{\phi^+}{\epsilon} + \frac{\partial^p \phi^+}{\partial y^p} = \frac{\phi^-}{\epsilon},$$

Crank-Nicholson:

$$\frac{\phi^+}{\epsilon} + \frac{1}{2}\frac{\partial^p \phi^+}{\partial y^p} = \frac{\phi^-}{\epsilon} - \frac{1}{2}\frac{\partial^p \phi^-}{\partial y^p},$$

for ϕ^+ as a function of y. Here the superscripts $+$ and $-$ denote evaluation at the current and previous x–position respectively, and ϵ is the streamwise step-length. We note that although the system which requires inversion to determine ϕ^+ is of the same form in both case, the extra accuracy comes from evaluating the $\frac{\partial^p \phi}{\partial y^p}$ at the mid-point and hence the streamwise derivative then becomes a centred difference. The only additional computation that results is involved in computing the term $\frac{\partial^p \phi^-}{\partial y^p}$ which is outweighed by the additional accuracy obtained. In all the calculations reported here a streamwise step–length of 0.1 was used.

The system is now discretized using a second order accurate (for the fourth derivative, this requires five points) finite difference scheme in the normal η coordinate which when combined with the Crank–Nicholson discretisation for the streamwise derivatives allows the system to be written in the form

$$a_n v_{n+2} + b_n v_{n+1} + c_n v_n + d_n v_{n-1} + e_n v_{n-2} + f_n u_{n+1} + g_n u_n + h_n u_{n-1} = R_n^{(v)}, \quad (3.1a)$$

and

$$\check{a}_n u_{n+1} + \check{b}_n u_n + \check{c}_n u_{n-1} + \check{d}_n v_n = R_n^{(u)}. \quad (3.1b)$$

Here the index n denotes evaluation at the nth normal grid–point, the terms on the left-hand-sides of these expression are evaluated at $x = x + \epsilon$ and the $R_n^{(u)}$ and $R_n^{(v)}$ denotes terms evaluated at the previous streamwise position. (For the sake of brevity the form of the coefficients in (3.1a,b) are not presented here; they can be obtained on application to the authors).

Here we highlight the major difference between the present scheme and that used in Hall (1983) (apart from the additional accuracy obtained in the present calculations due to the Crank–Nicholson discretisation of the streamwise derivatives). The method used in Hall (1983) is to move the terms in (3.1a) associated with u to the right hand side, hence evaluating them at the previous point, and then invert the penta–diagonal system for v. Using this solution it is then possible to solve the tri-diagonal system (3.1b) for u. Here we choose to invert the entire system in one calculation, thus preserving the structure of the system and rendering our scheme truly second order accurate in the streamwise coordinate. The method used for this inversion represents a modified form of a Davis Coupled Scheme and has been outlined in Otto & Bassom (1993) (the reader is referred to that paper for full details).

To monitor the growth (or decay) of an initial disturbance as the calculation proceeds downstream we define the energy as

$$E^{(\eta)} = \int_0^{\eta_\infty} \tilde{U}^2 d\eta.$$

If we define the growth rate as

$$\sigma = \frac{1}{E} E_x = \frac{E_x^{(\eta)}}{E^{(\eta)}} + \frac{1-n}{2x}, \tag{3.2}$$

then a neutral point is the x–station where the real part of the quantity σ, defined in (3.2), changes sign. The imaginary part of σ gives us the wavespeed in the streamwise coordinate. It should be noted that for the steady Görtler problem, $\Omega \equiv 0$, we have $\mathrm{Imag}(\sigma) \equiv 0$.

§4 Results and Discussion

In a preliminary report (Otto & Denier (1993a)) we presented some limited results concerning the effect of crossflow on the Görtler instability mechanism at $O(1)$ wavelengths; however several choices of various parameters were made which limits the

applicability of that study. Here we shall now endeavour to provide a fuller description of the effect of crossflow on the Görtler vortex instability mechanism.

In order to decrease the number of parameters in our study we will, throughout the calculations reported, fix the Görtler number and note that for larger Görtler numbers the results will be quantitatively similar to those presented here (keeping in mind that for larger Görtler numbers the flow becomes unstable at a smaller value of the streamwise variable x). The value chosen for the Görtler number is $G = 0.05$, this value is taken solely for convenience. The work of Hall (1983) clearly demonstrates, in the case of Görtler vortices in two–dimensional boundary layers, that the initial form of the perturbation, and the position at which it is imposed, are key factors in determining the stability characteristics of flow field. Not surprisingly such is the case in the present problem, however as we are predominantly concerned with the effect of both an imposed pressure gradient and crossflow we choose to ignore this effect and consider only the case when the initial perturbation is of the form

$$(\bar{U}, \bar{V}) = \left(\eta^6 e^{-\eta^2/\eta_{\mathrm{ext}}}, 0\right),$$

(note that this is precisely the form used by Hall (1983)). Here η_{ext} is a measure of the normal extent of the initial perturbation; for the sake of definiteness we choose $\eta_{\mathrm{ext}} = 4$ for all the calculations reported here. This condition is now imposed at $\bar{x} = 20$ and the numerical scheme described above is used to march the solution in x at each stage monitoring the growth rate σ of the disturbance. We note in passing that the value at which the initial perturbation is imposed was varied ($\bar{x} = 30$ and $\bar{x} = 40$); in all case the growth rate curves coalesce into the unique right-hand branch of the neutral curve far downstream. It is in this regime that the parallel flow approximation achieves validity, however as demonstrated by Hall (1982) this asymptotic regime can readily be described without recourse to this *ad hoc* approximation technique.

One of the major differences between this work and OD is that here we shall retain the variation of χ with x. Thus for each pressure gradient two forms of wall curvature will be considered; (*i*) $\chi \equiv 1$ (OD), and (*ii*) $\chi = x^{\frac{1-5n}{2}}/\bar{x}^{\frac{1-5n}{2}}$ (this being the wall curvature required to support Görtler vortices far downstream).

We consider first the effect that the modification of the basic flow due to the presence of the pressure gradient has upon the stability characteristics in the absence of the crossflow component of the basic flow. As was demonstrated by OD, in this case the most unstable mode is found to be steady; we therefore set $\Omega = 0$. In figure 1 we show three neutral curves for the cases $n = 1/20$, $n = 0$ and $n = -1/20$ for the choice (i) of

constant curvature; these correspond to a favourable–, no–, and an adverse–pressure gradients respectively. The results are presented in terms of the local Görtler number and local wavenumber which are defined as

$$G_x = Gx^{\frac{3-3n}{2}}, \qquad a_x = ax^{\frac{1-n}{2}}, \tag{4.1}$$

and have been derived with respect to the local boundary layer thickness. The neutral curves were generated by fixing the Görtler number $G = 0.05$ (see the discussion above), choosing a spanwise wavenumber a and marching the solution to (2.3a,2.7) downstream until such point at which the growth rate σ (given by (3.2)) changes sign. At this point the local Görtler number and local wavenumber can be calculated from (4.1). This procedure is then repeated for different values of spanwise wavenumber a to produce a curve of the form given in Figure 1.

In figure 2 we present the neutral curves for the curvature distribution (ii), again with $G = 0.05$. In both cases it is readily seen that for the case of a favourable pressure gradient the range of local wavenumber over which the flow is unstable is increased and, additionally, the minimum value of the local Görtler number G_x is decreased with increasing n. We note that this thickening of the neutral curve corresponds to an increase in the streamwise extent over which a disturbance of given wavenumber a is unstable. Thus, for the two representative curvature distributions considered here, it is the case of boundary layer with a favourable pressure gradient that is most susceptible to Görtler vortices. In the limit of large spanwise wavenumber a and large Görtler number G it is possible to describe, in a self consistent asymptotic setting, the structure of the Görtler vortex in the vicinity of the right–hand branch of the neutral curve. The details of the calculation relevant to the right-hand-branch of the neutral curve are given in the appendix at the end of this paper.

In figure 3 we present plots of the (scaled) growth rate, β^*, and the position of vortex activity, η^*, as a function of the scaled wavenumber σ^* for various values of n (see the appendix for the precise definition of these scaled quantities). From figure 3 we note, as found by Denier et al (1991), that $\beta^* \sim 1/\sigma^{*2}$ as $\sigma^* \to 0$; this fact can then be used to determine the most unstable Görtler vortex mode as in Denier et al. To clearly see the effect of changing the pressure gradient (by varying the parameter n) on the right-hand-branch of the neutral curve we present, in figure 4, a plot of the scaled neutral wavenumber σ^*, at which $\beta^* = 0$, together with the position of vortex activity η^*. As n decreases the scaled wavenumber σ^* decreases; thus a less favourable pressure gradient moves the right-hand-branch of the neutral curve to the

left. In this sense a boundary layer flow with a favourable pressure is more unstable to Görtler vortices. Similarly, for decreasing n, the position η^* at which the neutral vortex resides increases. Combining the results of our numerical calculations with the large wavenumber asymptotics which appear in the appendix we can clearly see that the range of local wavenumbers over which the disturbance is growing is increased and also the critical local Görtler number is decreased. This result is in stark contrast to the case of Tollmien–Schlichting waves in an external boundary layer where it has been demonstrated that an adverse pressure gradient is destabilizing (see Rosenhead (1963), Ch. IX). We conjecture that such a destabilization due to a favourable pressure gradient is due to the convective nature of the Görtler vortex instability. However, since the question of whether the Görtler vortex instability is convective or absolute is still undecided, although experimental observations do support the commonly held belief that it is in fact a convective instability, we believe that this point warrants further investigation, the results of which we hope to report in a forthcoming article.

We note, from figure 1 and 2, the apparent absence of a left–hand branch of the neutral curves. This arises due to the computational difficulty in obtain neutral values relevant to this branch due to the fact that exceptionally small values of the wavenumber a are required in such a calculation. At this point we emphasize that the evolution of a single mode of fixed spanwise wavenumber a the local wavenumber varies according to (4.1) as the calculation proceeds downstream. In this case the loci of local wavenumber is given by the dashed line in figure 2 and as such there is a finite interval in the streamwise direction for which σ_r is positive and the mode is growing in amplitude. In this interval we would then expect nonlinear terms to come into play and the results of Hall (1988), Otto & Bassom (1994b) and Denier & Hall (1993) become relevant. The loci shown in figure 2 is for the representative case $a = 0.185$; the solid block shows the position at which σ_r first changes sign and we note that this trajectory does not cross the right hand branch with the range of the current calculation (4000 steps of length 0.1 in x).

We now turn our attention to the effect of cross flow on the Görtler instability. In the asymptotic regime relevant to the right-hand branch of the neutral curve (ie large wavenumber a and large Görtler number G) Hall (1985) demonstrated that the effect of crossflow is to shift the right-hand branch of the neutral curve to the left. We will show that such an effect can be achieved even with the modest values of crossflow.

In our earlier study, Otto & Denier (1993a), the effect of crossflow was considered for the three forms of pressure gradients given above and it was shown that all cases were affected in a similar manner. For this reason we choose to consider only the

case of the favourable pressure gradient here as this is the most unstable in the sense described above. In figure 5 we show a different form of neutral curve, where we fix the wavenumber at $a = 0.195$ (with the other parameters as $n = 1/20$, $G = 1/5$ and $\chi \equiv 1$). These choices were made so that the calculation is in a parameter regime which is relevant to the right-hand branch of the neutral curve. In this case the "stability bubbles"are actually closed. Here we present results for increasing values of the crossflow parameter λ, the curves shown are for $\lambda = 0, 0.1, 0.2$. The triangular symbols depict the points at which the disturbance begins to grow, σ_r first becomes positive, and the circular symbols where it first begins to decay, σ_r becomes negative. We notice that the effect of increasing the crossflow parameter λ is to shift these curves rather than compressing them as might be expected from the earlier asymptotic results of Hall (1985) and Otto & Bassom (1993).

In order to explain this apparent discrepancy we revert to the other form of neutral curve, that is where we fix Ω and vary the wavenumber. One of the difficulties in comparing our results with the asymptotic predictions of previous authors is that we must, necessarily, fix the frequency of the disturbance at the outset for our numerical calculation. In figure 6 we show the calculation for $\Omega = 1/20$ with $\lambda = 1$ and $\Omega = \lambda = 0$ for $G = 1/20$, $\chi \equiv 1$ and $n = 1/20$. In this case the right-hand branch for the case with crossflow has been moved to the left, and now lies inside the neutral curve for the two-dimensional boundary layer case. However, we note that the critical neutral Görtler number is only slightly modified by the presence of the crossflow. Thus, although crossflow has an appreciable effect of the right-hand branch structure, a result that is apparent from the asymptotic results of Hall (1985) and Otto & Bassom (1993), it does not appear, on the basis of our calculations, to completely destroy unstable Görtler vortices. In particular, for a given flow situation conclusions concerning the instability of a curved boundary layer in the presence of crossflow can only be determined by solving the full governing equations (2.3) starting from some suitable initial condition.

To complete our discussion, in figure 7, we present the streamwise variation of the growth rate σ, for the particular choice of parameters $\lambda = 0.2$, $a = 0.195$, $G = 0.05$, $n = 1/20$ and $\chi \equiv 1$, from which we can readily see that the growth rate σ_r is positive over a large streamwise interval. Finally in figure 8 we show the contours of the real part of the normal perturbation velocity component $\tilde{V}$ at $z = 0$, and in figure 9 we shown the contours of the real part of $\tilde{V}$ at $\eta = 1$. Figure 8 clearly demonstrates the growth of the vortex motion as the calculation proceeds downstream and also highlights the presence of the imaginary part of the growth rate σ on the vortex motion while

from figure 9 we see the vortices migrate in the x–z plane as expected in the presence of crossflow.

§5 Conclusions

In this study we considered the effect of crossflow on the Görtler vortex instability mechanism. Perhaps just as important as the conclusions concerning crossflow, is the finding that the favourable pressure gradient flows lead to far more unstable Görtler modes, a fact that we contribute to the convective nature of the Görtler instabilities. We have limited ourselves to calculations in which the crossflow is small, this is necessary so that waves with spanwise wavelength comparable with the boundary layer thickness can be considered. It is found that the dominant effect of crossflow is to re-orientate the modes and change the streamwise extent over which they grow. In the conventional Görtler problem it is well known that the modes are steady, however in this three-dimensional case the 'most unstable' mode is not necessarily steady. We note that as the crossflow is further increased the modes start to grow after shorter streamwise distances, until the terms ∂_x^2 and $\partial\tilde{P}/\partial x$ become significant. The modes characteristics can then be determined only by solving the full linearized equations. In this case these modes can be thought of as crossflow modes modified by curvature. It is now accepted that good approximations to these equations can be found using a form of the, so called, Parabolised Stability Equations (PSE), see for example Bertolotti (1991). It is worth emphasising that the PSE are exact for the two-dimensional Görtler problem, since in this case the streamwise wavenumber is zero.

It would be interesting to determine how the crossflow will affect the receptivity of a situation to Görtler vortices. We presume that the 'extra' shear caused by the presence of the crossflow will increase the receptivity coefficient. In a recent review article by Bassom & Seddougui (1994), the receptivity coefficient, which is a measure of the coupling between an external perturbation (for example, in the form of an isolated surface roughness element) and the resulting flow disturbance, was calculated for the most unstable Görtler vortices and it was found to increase with increasing crossflow. Such a receptivity calculation would in a similar fashion to that presented by Denier, Hall & Seddougui (1991), using the modifications to the initial conditions recently proposed by Bassom & Hall (1994).

Another interesting question concerns the effect that the crossflow will have on the secondary stability of a boundary layer which has been perturbed by the presence of a Görtler vortex. In Hall & Horseman (1991) and Otto & Denier (1993b), the temporal

inviscid stability of two nonlinear vortex states were considered, derived in Hall (1988) and Otto & Bassom (1994b) respectively. In the present calculation we have only a linear vortex state however the stability of the boundary layer with this imposed vortex motion can still be analysed. In the case of a Görtler vortex in the presence of a small crossflow the problem of the secondary instability can be posed in an asymptotically rigorous setting and the resulting three-dimensional Rayleigh equation can be solved using the methods developed in Otto & Denier (1993b). The results of the study of Otto & Denier (1993b) have demonstrated the existence of three inviscid modes which can lead to the flow's breakdown. Firstly there are the even and odd modes, which give rise to the horseshoe and wavy vortices respectively. There is also a second even mode which has a larger temporal growth rate and persists over a larger range of secondary streamwise wavelengths. This mode has a large second harmonic component the magnitude of which is actually equal to that of the first harmonic at the wall. A similar mode has also been observed in stability of the flow in a corner flow by Dhanak (1993). Studies of both the receptivity and secondary instability problem are currently underway and we hope to report on the results of these studies in the near future.

References

Bassom, A. P. & Hall P. (1991) Vortex instabilities in three–dimensional boundary layers: The relationship between Görtler and Crossflow vortices. *J. Fluid Mech* **232** 647

Bassom, A. P. & Hall P. (1994) The receptivity problem for $O(1)$ wavelength Görtler vortices *Proc. Roy. Soc. Lond. A. (in press)*

Bassom, A. P. & Otto, S. R. (1993) Weakly nonlinear stability of viscous vortices in three–dimensional boundary layers. *J. Fluid Mech.* **249** 185

Bassom, A. P. & Seddougui, S. O. (1994) Receptivity mechanisms for Görtler vortex modes . *submitted to Theor. Comp. Fluid Dynamics*

Bertolotti, F. P. (1991) Linear and Nonlinear Stability of Boundary Layers with Streamwise Varying Properties. *PhD Thesis, The Ohio State University*

Cooke, J. C. (1950) The boundary layer of a class of infinite yawed cylinders *Proc. Camb. phil. Soc.* **46** 645

Denier, J.P., Hall, P. & Seddougui, S. (1991) On the receptivity problem for Görtler vortices: vortex motion induced by wall roughness *Phil. Trans. Roy. Soc. Lond. A* **335** 51

Dhanak, M. (1993) Private Communication

DiPrima, R. C. & Pridor A. (1979) The stability of viscous flow between rotating concentric cylinders with an axial flow *Proc. R. Soc. Lond. A* **366** 555

Falkner, V. M. & Skan, S. W. (1930) Some approximate solutions if the boundary layer equations *Rep. Memor. aero. Res. Coun., Lond. No. 1914*

Goldstein, S. (1948) On laminar boundary layer flow near a position of separation. *Q. J. Mech.* **1** 43

Görtler, H. (1940) On the three dimensional instability of laminar boundary layers on concave walls *NACA Tech. Memo no. 1375*

Gray, W. E. (1952) The nature of the boundary layer at the nose of a swept back wing *Unpublished work Min. Aviation Lond.*

Gregory, N., Stuart, J. T. & Walker, W. S. (1955) On the stability of three-dimensional boundary layers with application to the flow due to a rotating disk *Phil. Trans. R. Soc. Lond. A* **248** 155

Hall, P. (1982) Taylor–Görtler vortices in fully developed or boundary layer flows. *J. Fluid Mech.* **124** 475

Hall, P. (1983) The linear development of Görtler vortices in growing boundary layers. *J. Fluid Mech.* **130** 597

Hall, P. (1985) The Görtler vortex instability mechanism in three–dimensional boundary layers. *Proc. Roy. Soc. Lond. A* **399** 135

Hall, P. (1988) The nonlinear development of Görtler vortices in growing boundary layers *J. Fluid Mech.* **193** 247

Hall, P. (1990) Görtler vortices in growing boundary layers: the leading edge receptivity problem, linear growth and the nonlinear breakdown stage *Mathematika* **37** 151

Hall, P. & Horseman, N. J. (1991) The inviscid secondary instability of fully nonlinear longitudinal vortex structures in growing boundary layers *J. Fluid Mech* **232** 357

Hall, P. & Morris, H. (1991) On the stability of boundary layers on heated flat plates *J. Fluid Mech* **245** 367

Macaraeg, M. G., Streett, C. L. & Hussaini, M. Y. (1988) A Spectral Collocation Solution to the Compressible Stability Eigenvalue Problem. *NASA technical Paper* **2858**

Otto, S. R. & Bassom, A. P. (1993) An Algorithm for Solving the Viscous Equations Arising in the Stability of Three-Dimensional Centrifugal Instabilities *ICASE Internal Report, 98*

Otto, S. R. & Bassom, A. P. (1994a) The effect of crossflow on Taylor vortices. *Quart. J. Mech. Appl. Math. (in press)*

Otto, S. R. & Bassom, A. P. (1994b) Nonlinear development of viscous Görtler vortices in a three dimensional boundary layer *Stud. Appl. Math, in press*

Otto, S. R. & Denier, J. P. (1993a) Concerning the effect of crossflow in the stability of Görtler vortices, in the Proceedings of the ICASE, NASA LARC workshop on Transition, Turbulence and Combustion *herein referred to as OD*

Otto, S. R. & Denier, J. P. (1993b) On the Secondary Instability of the Most Dangerous Görtler Vortex, in the Proceedings of the IUTAM symposium on the Nonlinear instability of Non-parallel flow, Potsdam, NY, USA

Rosenhead, L., *Laminar Boundary Layers*, (Dover, New York, 1963)

Taylor, G.I. (1923) Stability of a viscous liquid contained between two rotating cylinders *Phil. Trans. R. Soc. Lond. A* **223** 289

Zurigat, H. & Malik, M. R. (1993) Effect of Crossflow on Görtler instability, in the Proceedings of the ICASE, NASA LARC workshop on Transition, Turbulence and Combustion

Appendix

Here we present some details concerning the effect of the pressure gradient on the Görtler instability mechanism. Noting that the results presented in §3 are relevant to the case when both the wavenumber a and the Görtler number G are $O(1)$ quantities we will restrict our attention to the case of the large Görtler number limit.

To proceed we consider first the asymptotic regime appropriate to the right-hand-branch of the neutral curve (we will follow closely the work of Denier et al (1991); the reader is referred to that paper for full details). Thus, setting $\lambda = \Omega = 0$ in (2.3a,2.7) we seek solutions in the limit $G \to \infty$ with $a = O(G^{1/4})$. Thus writing

$$a = \sigma G^{1/4} \tag{A.1}$$

we seek a solution of (2.3a,7) confined to a layer of depth $k^{-1/2} \sim G^{-1/8}$ centred on the location $y = \bar{y}(x)$. The appropriate expansion is given by

$$u = \left\{ u_0(x,\xi) + k^{-1/2} u_1(x,\xi) + \cdots \right\} \exp\left[G^{1/2} \int \beta(x) dx \right],$$

where $\xi = \sigma^{1/2} G^{1/8} (y - \bar{y})$. The eigenrelation is then found to be given by

$$\left[(\overline{u}\beta + \sigma^2)^2 - \chi \overline{u}\, \overline{u}_y \right] |_{y=\bar{y}} = 0, \tag{A.2}$$

together with the condition that ensures the vortex is confined to the layer centred on $y = \bar{y}$;

$$\frac{\partial}{\partial y} \left[(\overline{u}\beta + \sigma^2)^2 - \chi \overline{u}\, \overline{u}_y \right] |_{y=\bar{y}} = 0. \tag{A.3}$$

Thus the conditions (A.2) and (A.3) serve to determine both the growth rate β and the position $\bar{y}$ as a function of the scaled wavenumber σ. For the self–similar boundary layer (2.2a) we have $\bar{u} = x^n f'(\eta)$, where $\eta = y/x^{\frac{1-n}{2}}$. Writing

$$\beta = \beta^* \left(\chi x^{\frac{n-1}{2}} \right)^{1/2}, \qquad \sigma = x^{n/2} \left(\chi x^{\frac{n-1}{2}} \right)^{1/4} \sigma^* \tag{A.4}$$

the eigenrelation (A.2) together with (A.3) can be rewritten as

$$(f'\beta^* + \sigma^{*2})^2 = f' f'', \quad 2f''\beta^*(f'\beta^* + \sigma^{*2}) = (f'f'')' \tag{A.5}$$

where f' is to be evaluated at some position η^* where (A.5b) holds. We note that n does not appear explicitly in (A.5); its presence is felt through the effect on the

boundary later profile f (see (2.2a)). Plots of β^* versus σ^* are given in the text of the paper.

Here we note that there a a critical value of $n = n_c < 0$ at which the boundary layer equations (2.2) no longer yield physically relevant solutions; indeed at this point we have $f''(0) \to 0$ as $n \to n_c$. For $n < n_c$ the boundary layer equations then predict solutions which have a finite region of separated flow for all values of the streamwise coordinate x; such a solution is of no physical relevance.

To complete the description of the wavenumber spectrum for Görtler vortices in the large Görtler number limit we can follow Denier et al (1991) and consider the inviscid Görtler vortex modes which lie in the parameter regime $G \gg 1$ with $a = O(1)$. In this case there is an exact solution of the linearized governing equations (see Denier et al (1991) for full details) in which the growth rate $G^{-1/2}\beta$ is given by

$$G^{-1/2}\beta = \frac{a\chi}{2},$$

which depends only on the curvature and the spanwise wavenumber. Thus the growth rate of the inviscid Görtler vortex is unaffected by the presence of a pressure gradient; note however, that the normal structure of the inviscid mode is affected due to its *dependence on the basic flow* $\overline{u}$ *(see* Denier et al (1991)). It is then the inviscid regime which represents a "turning point" with respect to the effect of pressure gradient on the Görtler vortex instability. For $a \gg 1$ (with $G \gg 1$) a favourable pressure gradient destabilizes the flow whereas for $a \ll 1$ (again with $G \gg 1$) a favourable pressure gradient stabilizes the flow. This last point can be derived from the small wavenumber asympotitics presented in Hall & Morris (1992) and is left as an exercise for the interested reader.

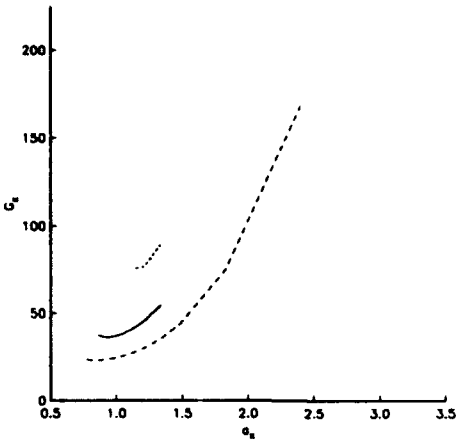

Figure 1: Neutral curves for case (i), with $n = 1/20$, 0 and $n = -1/20$, they curves appear in ascending order, that is the highest curve corresponds to $n = -1/20$.

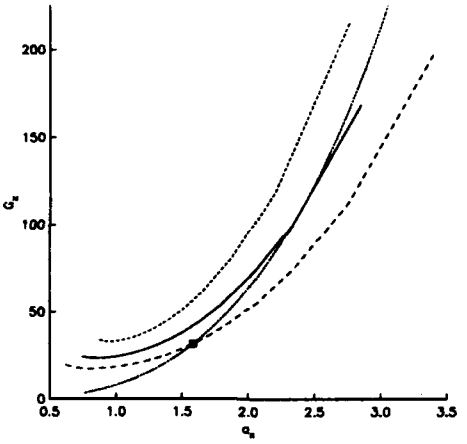

Figure 2: Neutral curves for case (ii), with $n = 1/20$, 0 and $n = -1/20$, they curves appear in ascending order.

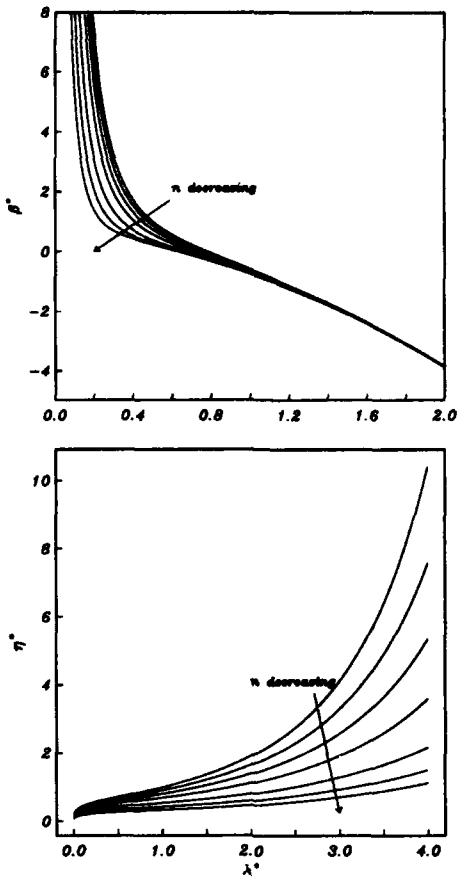

Figure 3: Plots of scaled growth rate β^* and the position of vortex activity η^* versus the scaled wavenumber σ^* (see appendix for details).

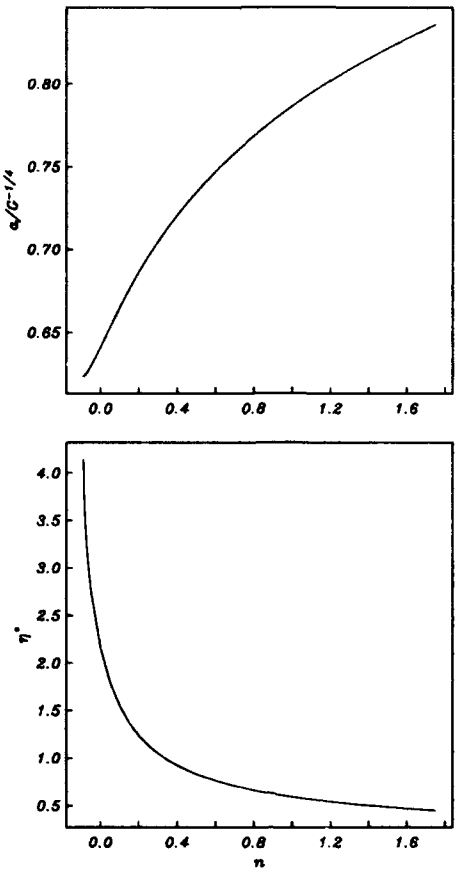

Figure 4: Plot of scaled neutral wavenumber σ^* and the position of vortex activity versus the parameter n (see appendix for details).

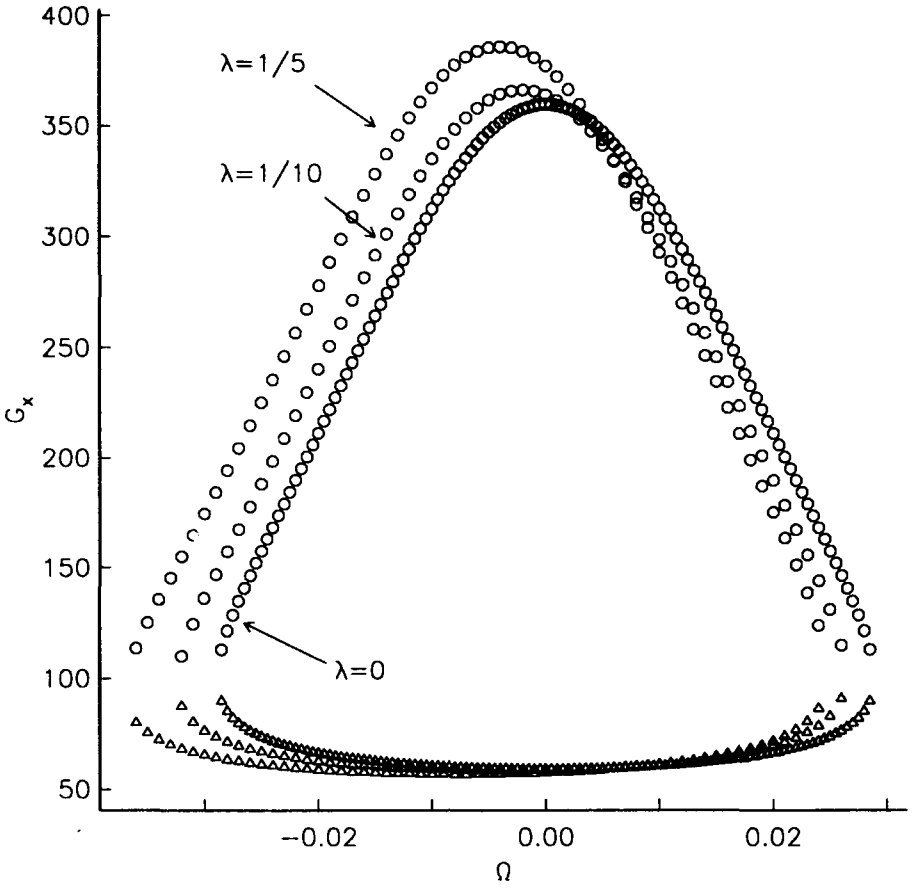

Figure 5: Stability Bubble for case close to the right hand side of the neutral curve.

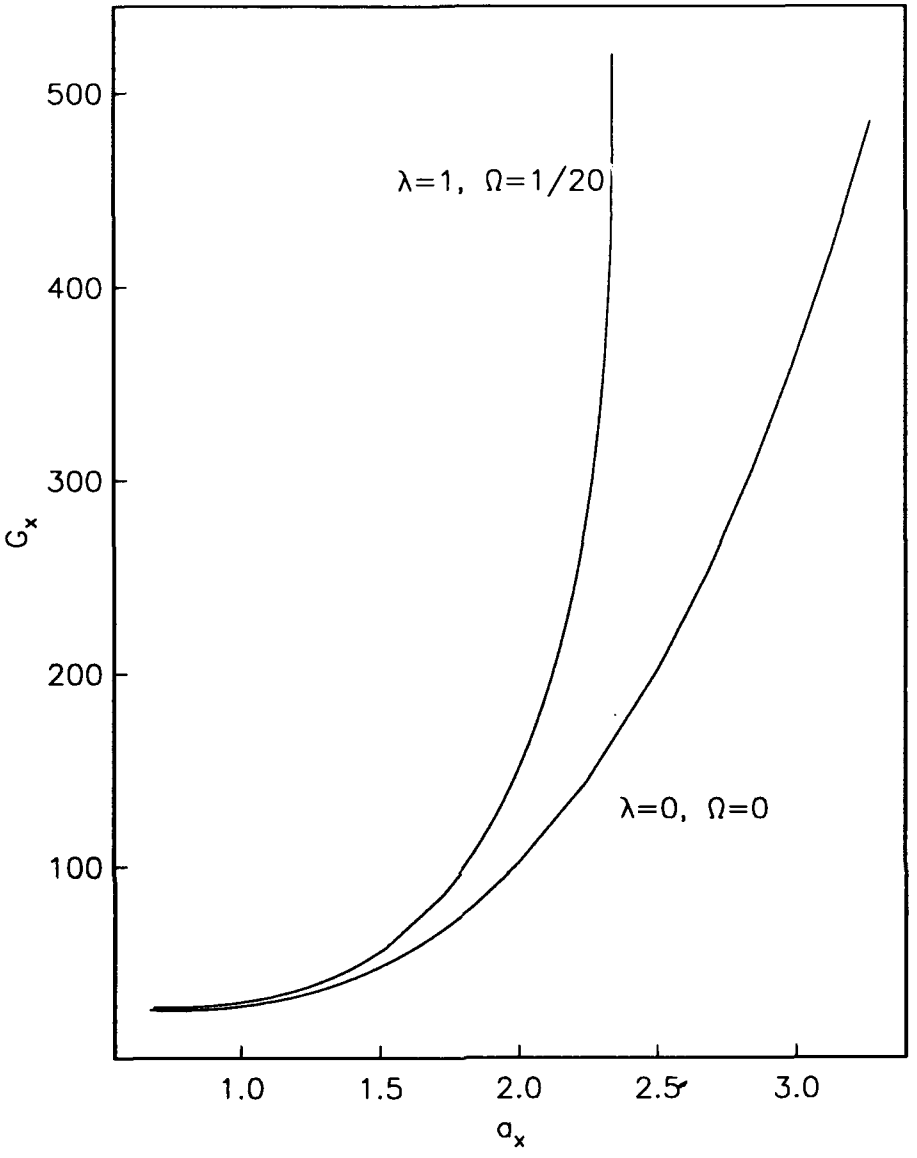

Figure 6: Neutral curves for $\Omega = 1/20$, with $\lambda = 0$ and $\lambda = 1$.

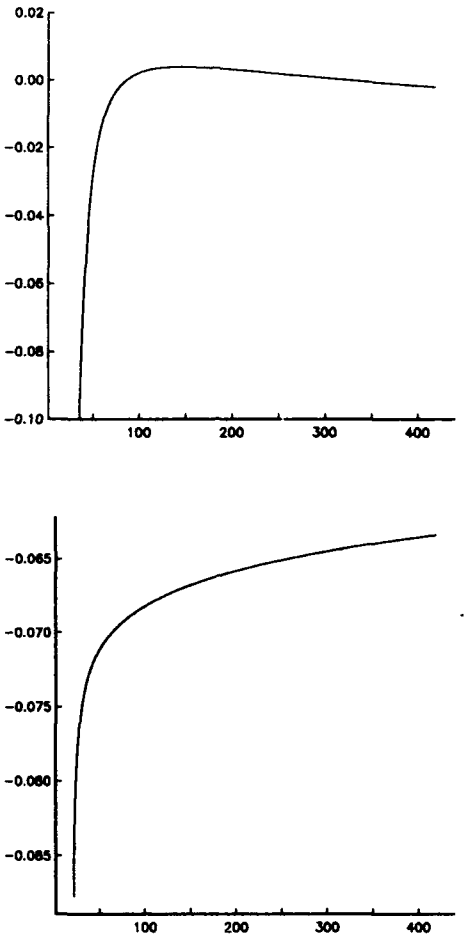

Figure 7: The Real and Imaginary Parts of σ versus x for an unsteady case with crossflow.

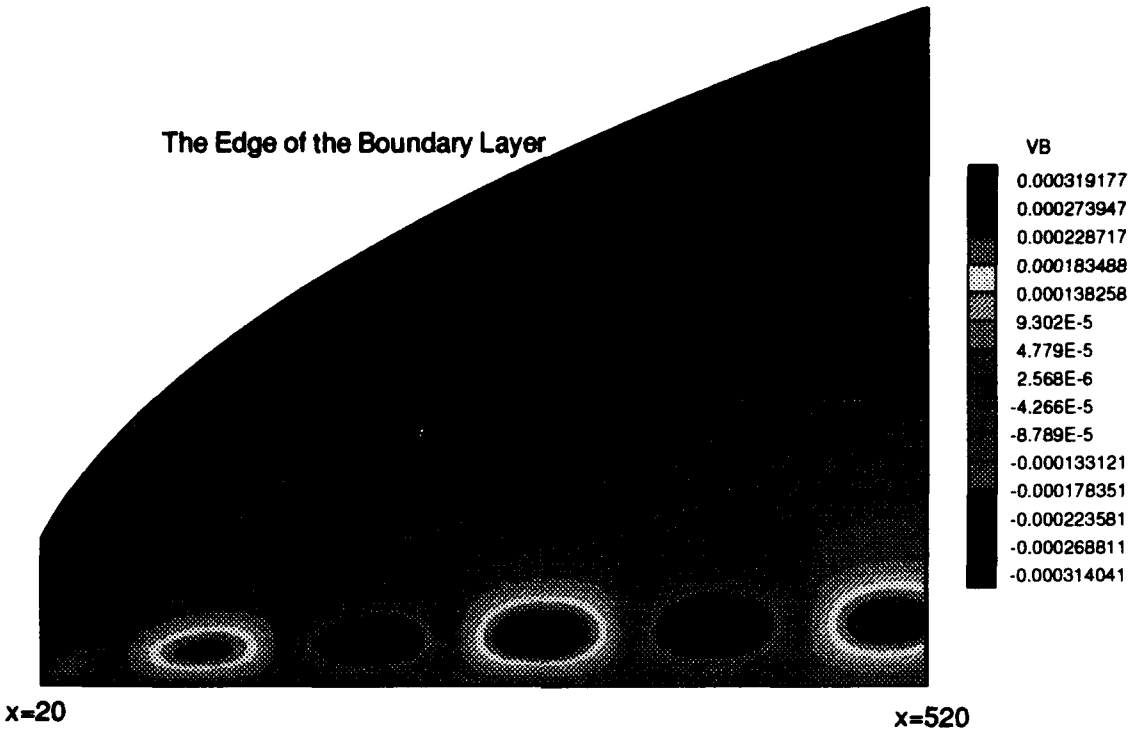

Figure 8: Contours of the real part of $\tilde{V}$ at $z = 0$.

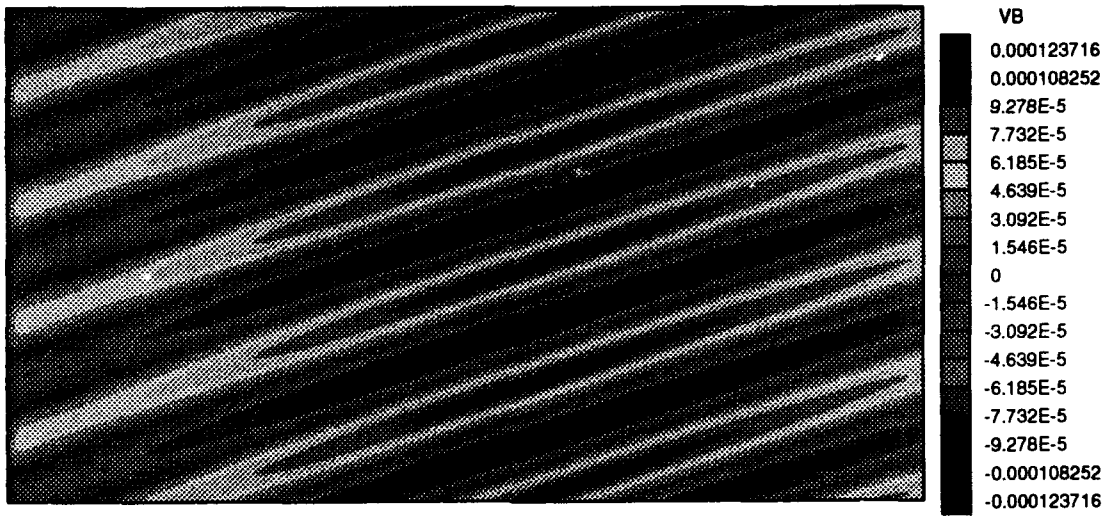

Figure 9: Contours of the real part of $\tilde{V}$ at $\eta = 1$ showing four completer periods in z.

REPORT DOCUMENTATION PAGE

Form Approved
OMB No. 0704-0188

1. AGENCY USE ONLY *(Leave blank)*	2. REPORT DATE	3. REPORT TYPE AND DATES COVERED
	March 1994	Contractor Report

4. TITLE AND SUBTITLE
THE EFFECT OF CROSSFLOW ON GÖRTLER VORTICES

5. FUNDING NUMBERS
C NAS1-19480
WU 505-90-52-01

6. AUTHOR(S)
S. R. Otto
James P. Denier

7. PERFORMING ORGANIZATION NAME(S) AND ADDRESS(ES)
Institute for Computer Applications in Science
and Engineering
Mail Stop 132C, NASA Langley Research Center
Hampton, VA 23681-0001

8. PERFORMING ORGANIZATION REPORT NUMBER
ICASE Report No. 94-19

9. SPONSORING/MONITORING AGENCY NAME(S) AND ADDRESS(ES)
National Aeronautics and Space Administration
Langley Research Center
Hampton, VA 23681-0001

10. SPONSORING/MONITORING AGENCY REPORT NUMBER
NASA CR-194897
ICASE Report No. 94-19

11. SUPPLEMENTARY NOTES
Langley Technical Monitor: Michael F. Card
Final Report
Submitted to Journal of Fluid Mechanics

12a. DISTRIBUTION/AVAILABILITY STATEMENT
Unclassified–Unlimited

Subject Category 34

12b. DISTRIBUTION CODE

13. ABSTRACT *(Maximum 200 words)*

It is well known that the boundary layer flow over a surface with a region of concave curvature is susceptible to centrifugal instabilities in the form of Görtler vortices. In the limit of large Görtler number (a parameter which is a measure of the curvature of the surface) the effect of a crossflow component in the underlying basic flow has been shown to stabilises these modes and thus render the Görtler vortex mechanism inoperable in these situations. Here we consider the effect of crossflow when the Görtler number (and the scaled spanwise wavenumber of the vortex) are both order one quantities. The parabolic partial differential equations governing the linear evolution of a Görtler vortex in a three-dimensional boundary layer are solved numerically. Our results suggest that, at least for small magnitude crossflows, the Görtler vortex instability mechanism is still operable. In addition we consider the effect of an applied pressure gradient within the boundary layer on the instability mechanism and demonstrate that a favourable pressure gradient renders the boundary layer more susceptible to the Görtler vortex instability; this is in stark contrast to the case of Tollmien-Schlichting waves where a favourable pressure gradient stabilises the flow.

14. SUBJECT TERMS	15. NUMBER OF PAGES
Görtler, crossflow, pressure gradient	30
	16. PRICE CODE A03

17. SECURITY CLASSIFICATION OF REPORT	18. SECURITY CLASSIFICATION OF THIS PAGE	19. SECURITY CLASSIFICATION OF ABSTRACT	20. LIMITATION OF ABSTRACT
Unclassified	Unclassified		